Fracture Mechanics of Concrete Structures,
Proceedings FRAMCOS-2, edited by Folker H. Wittmann,
AEDIFICATIO Publishers, D-79104 Freiburg (1995)

SIZE EFFECT ON STRENGTH AND DEFORMATION OF RC BEAMS FAILING IN FLEXURE

H. Adachi, N. Shirai, and M. Nakanishi,
College of Science and Technology, Nihon University, Tokyo, Japan
K. Ogino
Taisei Corporation , Tokyo, Japan

Abstract

It has been pointed out that strength and deformability of reinforced concrete beams depend on its size. The purposes of this study are first to clarify various factors influencing the size effect phenomenon by numerical approach and secondly to verify Hillerborg's assumption by conducting experimental tests. Based on the results of the numerical investigation, various factors affecting the size effect phenomenon were clarified. Furthermore, the test results indicated that the size of specimens has a significant effect on the strength and deformability of reinforced concrete beams failing in flexure.

1 Introduction

It has been known that the shape of the descending branch after the peak stress of the stress-strain curve of concrete is affected by the specimens' size. Similarly, size effect has also been observed in reinforced concrete (RC) beams. One of the probable causes of size effect on the behavior of RC beams is the localization of strain in the compression zone. This

phenomenon was used by Hillerborg as the basis to explain the size effect on strength and deformability of RC beams. In this study, elastoplastic analysis of RC beam by one dimensional finite element method ; i.e., the fiber method, was conducted to investigate the size effect on the strength and deformability of RC beams. In the analysis, the size effect was considered by incorporating the stress-strain curve of concrete based on Hillerborg's assumption. In addition, four-point loading test on similarly differently scaled RC beams was conducted to examine the actual changes in the member behavior as the size of the beam is changed. The test results were compared with the analytical results.

2 Analysis of RC beams

2.1 Stress-strain relationship based on Hillerborg's assumption

Hillerborg (1988,1989) proposed a stress-strain relationship for concrete under uniaxial compression in terms of fracture mechanics concept. Fig.1 shows the representation of the concept of this relationship. The ascending branch up to the peak stress is shown in Fig.1(a) and the descending branch is shown in Fig.1(b). The complete stress-strain curve is shown in Fig.1(c). The ultimate average strain, $\overline{\varepsilon u}$, in Fig.1(c) is expressed by the following equation:

$$\overline{\varepsilon u} = \varepsilon_0 + wu/L \qquad (1)$$

Where "εo" in Fig.1(a) is the strain corresponding to the residual strain when $\sigma c=0$ in the unloading branch and "wu" in Fig.1(b) corresponds to the deformation when $\sigma c=0$ in the descending branch.

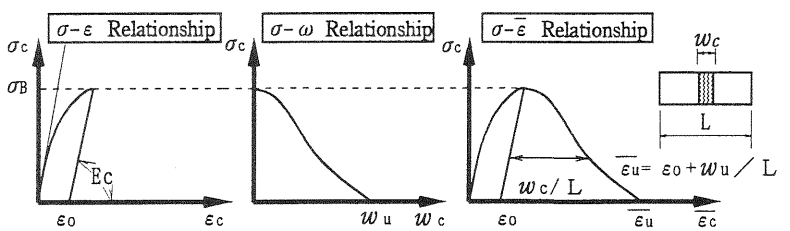

(a) Ascending branch up to peak stress (b) Descending branch after peak stress (c) Relationship of complete stress-strain of curve

Fig.1 Stress–Strain curve based on Hillerborg's assumption

2.2 Application to RC beams

In this section, Hillerborg's assumption is applied to the behavior of concrete at the compressive zone of the beam. The idealization of compressive zone

is shown in Fig.2. If the stress-strain relationship of concrete along the member axis follows the behavior of concrete cylinder, then Eqn.1 may be applied to express the stress-strain relationship of concrete at the compressive zone of the beam. Hillerborg simplified the ultimate strain in the descending branch, $\overline{\varepsilon u}$, by neglecting the strain εo in Eqn.1 as follows:

$$\overline{\varepsilon u} = wu / L \qquad (2)$$

Hillerborg assumed that the height of the compressive zone "c" is equal to gage length "L". Furthermore, he assumed that the additional deformation "wu" is a constant value; that is, 3 mm for normal strength concrete and 1 mm for high strength concrete. With these assumptions, it follows that the descending branch of the stress-strain curve highly depends on the length of the compression zone of the beam. Therefore, the deformability of the beam tends to become brittle as the depth of the beam becomes deeper. On the other hand, it is clearly seen that as the depth of the beam becomes shallower, the slope of the descending branch falls gentler.

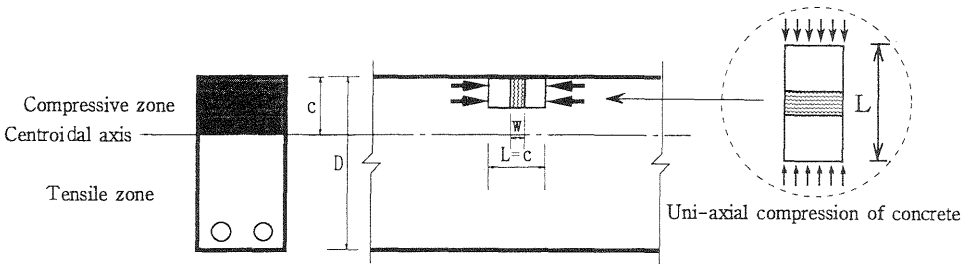

Fig.2 Concept of Compressive zone in RC beam

2.3 Elastoplastic analysis of RC beams

Elastoplastic analysis of RC beams was carried out to evaluate the size effect on strength and deformability. The adopted analytical procedure is the fiber method which is regarded as a simplified 1-D finite element method . The stress-strain relationship for concrete is evaluated by using a parabolic curve up to the peak stress and a straight line for the softening range. The stress-strain relationship for the reinforcement is evaluated by a bilinear model. Analytical variables are the depth of the beams "D" (1200 mm, 1000 mm, 800 mm, 600 mm, 400 mm, 200 mm, 100 mm, and 60 mm for a total of 8 cases) and the tensile reinforcing ratio "Pt" (4.2%, 3.5%, 2.8%, 2.1%, and 1.4% for a total of 6 cases) . A total of 48 cases were analyzed.

Fig.3 shows the relationship between the normalized bending moment ($M/BD^2\sigma_B$) and normalized curvature (ϕD). Where M is the bending moment, σ_B the compressive strength of concrete, B the width of beam and ϕ the curvature. Figs.4(a) and 4(b) show the normalized curvature (ϕD) - depth (D) and the normalized bending moment ($M/BD^2\sigma_B$) - depth (D) relationships, respectively. In these figures, the curvature and bending moments were normalized with respect to the corresponding values for the beam with the depth of 1200 mm. It is seen that the normalized bending moment of the beam with higher Pt increases as D becomes smaller. Similarly, the curvature tends to increase as the depth decreases, especially when Pt value is small. Consequently, it can be said that the size effect becomes more pronounced as the depth of the beams becomes shallower.

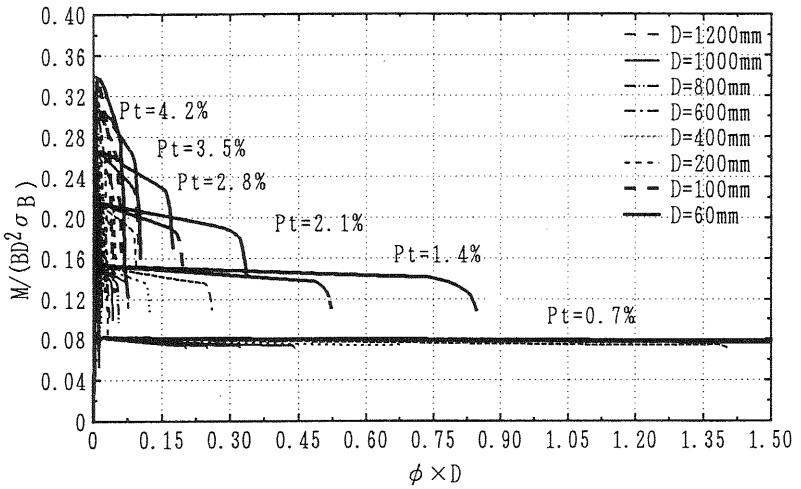

Fig.3 Normalized bending moment–normalized curvature curves

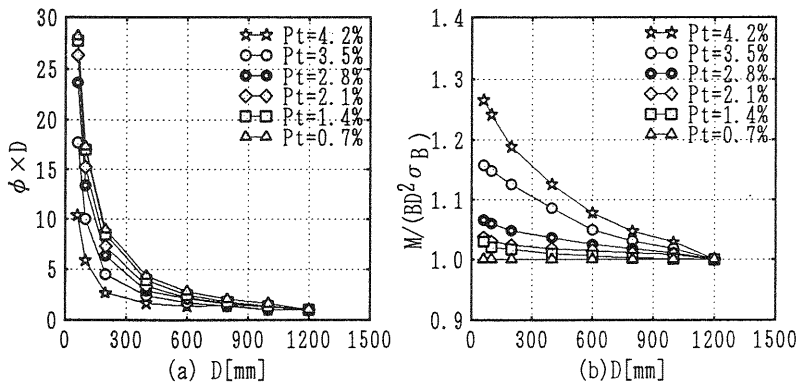

Fig.4 Normalized curvature–depth and bending moment–depth relationships

3 Experimental tests of RC beams

3.1 Specimens

Two series of tests; namely B07 and B21, were conducted. A total of eight RC beams with a single layer of tension reinforcement were prepared and tested to verify the size effect on the behavior of RC beams. The configuration and bar arrangement of the specimens are shown in Fig.5 and their structural variables are listed in Table 1. The tensile reinforcing ratios of B07 and B21 series are 0.7% and 2.1%, respectively. In both series, the cross-section of the full-scaled beam (s=1/1) is BxD = 300 mm x 600 mm and the length (l) is 5400 mm. The other specimens are 1/2, 1/4, and 1/8-scaled of the full-scaled specimen. In each series, the specimens were so designed that the mechanical reinforcement ratio (Pt σ_{sy} /σ_B) is constant. Where σ_{sy} is the yield strength of tension reinforcement. The mechanical properties of concrete and reinforcing bars are listed in Tables 2 and 3, respectively.

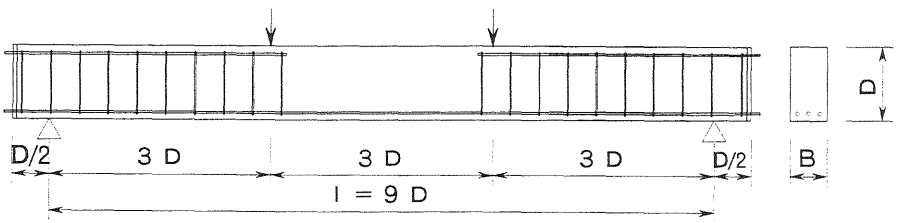

Fig.5 Configuration and ber arrangement of specimen

Table.1 Structural variables

Name of Specimen	Size of Specimen B×D×l(l')(mm)	Tensile Reinforcemnt	Pt (%)	$Pt \cdot \frac{\sigma_{sy}}{\sigma_B}$
B071	300×600×5400(6000)	4-D19	0.72	0.10
B211		6-D25	1.89	0.27
B072	150×300×2700(3000)	3-D10	0.53	0.09
B212		6-D13	1.90	0.27
B074	75×150×1350(1500)	2-D6	0.64	0.10
B214		5-D6	1.52	0.27
B078	37.5×75×675(750)	3-D3	0.84	0.09
B218		5-D4	2.50	0.28

B:width, D:depth, l:Span, l':Total length, Pt:Tensile reinforcing ratio,
$Pt \cdot \sigma_{sy} / \sigma_b$:mechanical reinforcement ratio

Table.2 Mechanical properties of concrete

Cylinder Size (mm)	Material Age	Compressive Strength σ_B(MPa)	Maximum Strain ε_B(%)	Elastic Coefficient Es(MPa)
5ϕ ×100	48	32.7	0.32	22.4×10^3
10ϕ ×200		28.4	0.31	19.6×10^3

Table.3 Mechanical properties of reinforcing bars

Reinforcement Diameter	D25	D19	D13	D10	D6	D4	D3
Yield Strength σ_y(MPa)	361	385	378	364	439	348	368
Tensile Strength σ_t (MPa)	570	566	551	503	561	485	497

The same ordinary Portland cement and river sand with maximum size of 2.5 mm were used irrespective of the specimens' size.

3.2 Loading and measurement system

Fig.6 shows the test setup and measurement system for the full-scaled RC beam specimen. The beams were simply supported and were subjected to two point loading by means of oil jacks. The deformation of the specimens were measured by means of displacement transducers at the mid span and at the loading points. The axial deformation over eight intervals along the compressive and tensile sides of the full-scaled and 1/2-scaled specimens were measured by means of clip gages to determine curvature distribution along the member axis. In the case of 1/4 and 1/8-scaled specimens, axial deformations were measured over four intervals by means of strain gages. Strain in the longitudinal bars were measured by means of strain gages at the mid span and at the loading points of the specimens.

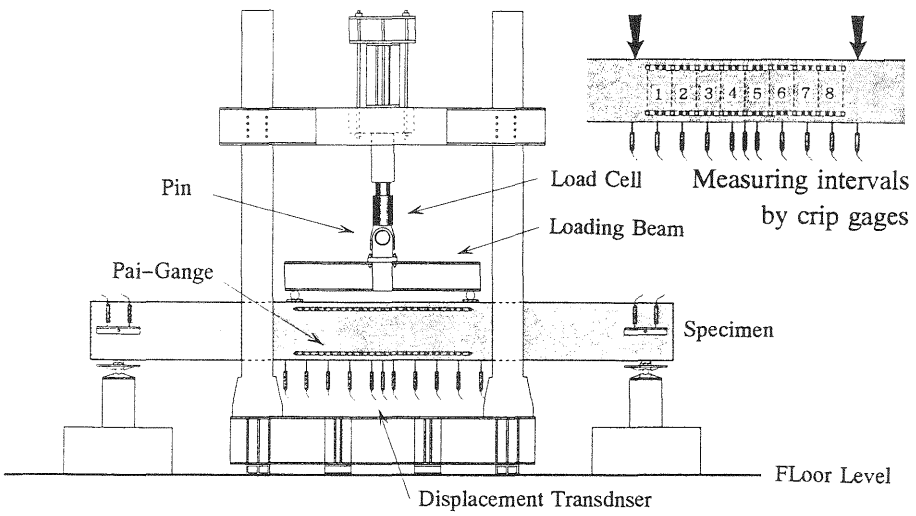

Fig.6 Loading and setup measurement system

4 Test results

4.1 Failure patterns

Fig.7 shows the failure pattern of each specimen. All specimens indicated a typical flexure-compression failure. Differences in crack patterns were observed for different beam sizes; that is, the number of cracks was more and the spacing between cracks was narrower in larger specimens. Furthermore, more cracks were developed and the length of cracks were shorter in beams with higher reinforcing ratio than those in beams with lower reinforcing ratio.

In the case of beams with higher reinforcing ratio, the zone of compression fracture extended beyond the centroidal depth.

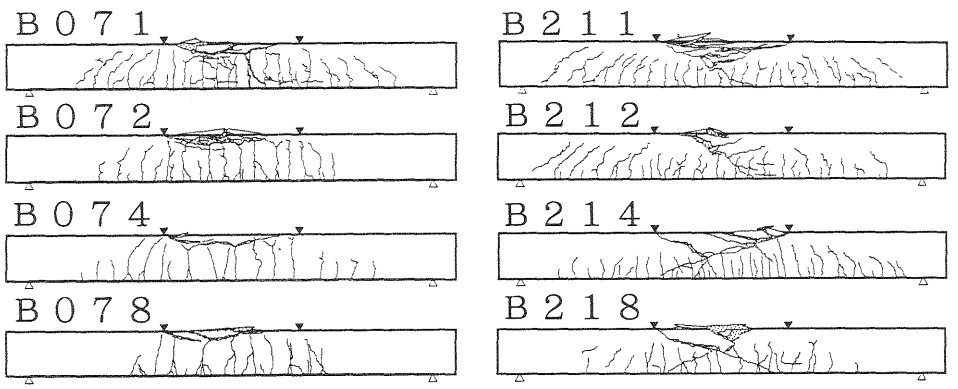

Fig.7 Failure Patterns of specimens

4.2 Strength and deformation

The test results are listed in Table 4. The normalized bending moment (M/BD^2) - member rototional angle (δ/l) relationships are shown in Fig.8. The maximum displacement, δmax, tabulated in Table 4 is defined as the displacement when the strength suddenly decreased as indicated by the encircled points in Fig.8. Shown in Fig.9 is the relationship between the maximum member rotational angle (δ_{max}/l) and D. There was no significant difference between the experimentally and analytically obtained yield strengths as indicated by the ratio Py/Pycal for different size of beam and reinforcement ratio. It can be seen from Figs.8 and 9 that the smaller specimen exhibits better deformability. This tendency is more pronounced in specimens with lesser tensile reinforcing ratio.

Table.4 Test Results

Specimen	Py (KN)	Pycal (KN)	Py/Pycal	Pu (KN)	Pu/Py	δ max (mm)	δ /l
B071	231.67	237.16	0.98	253.82	1.10	102.49	0.038
B072	45.86	41.16	1.11	52.23	1.14	95.91	0.071
B074	15.68	14.70	1.07	19.80	1.26	56.55	0.084
B078	4.12	4.21	0.98	5.19	1.26	35.02	0.104
B211	515.68	588.98	0.88	540.96	1.05	48.30	0.018
B212	140.63	154.84	0.98	145.82	1.04	29.20	0.022
B214	35.18	37.24	0.94	39.30	1.12	22.20	0.033
B218	10.68	11.76	0.91	11.66	1.09	13.01	0.039

Py:Yield load, Pycal:Calcurated yield load by "0.9• σ ₛᵧ •aₜ •d"
Pu:Maximum load, δ max:Maximum displacement, δ /l:Member rotational angle

4.3 Localization of curvature

Fig.10 shows the M-ϕ relationships in each interval (refer to Fig.6) evaluated from measured deformation along the compressive and tensile sides of the 1/1-scaled and 1/2-scaled specimens. In the case of 1/2-scaled specimens (B072, B212) and 1/1-scaled specimens (B071, B211), the curvature on each interval increases monotonically up to the yield strength. After the yield strength, the curvature at the fracture zone increases while those of the other zones decrease, indicating unloading. This tendency is noticeable after the ultimate strength.

4.4 Comparison between test and analytical results

Fig.11 shows the comparison between the experimental and analytical load-displacement curves. The analysis was repeated by changing the value of

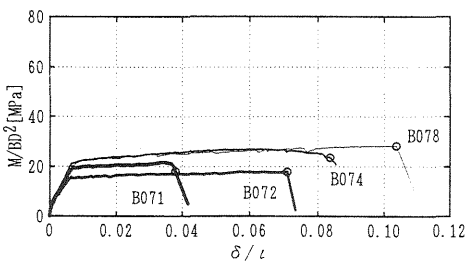

Fig.8 Normalized bending moment–displacement curves

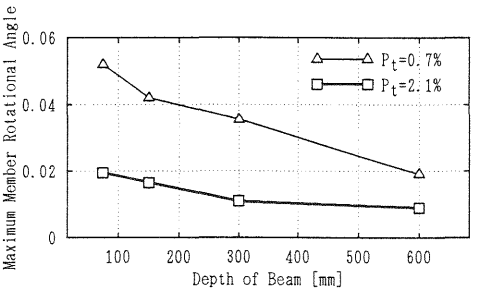

Fig.9 Maximum member rotaional angle–depth relationship

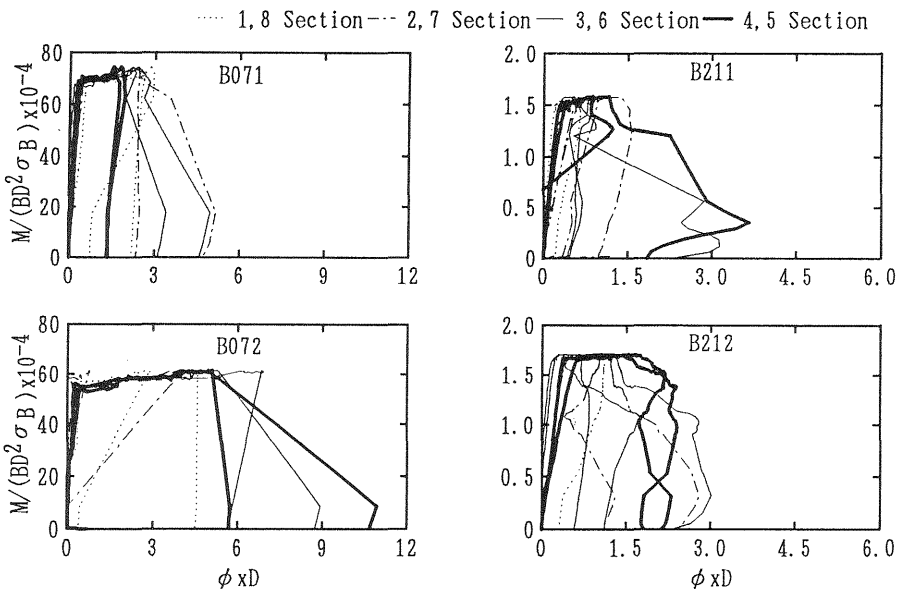

Fig.10 Normalized M – ϕ relationship

"wu" until a good fit with the test result was obtained. Shown in Fig.12 are the best fit values of "wu" plotted against D. The results of fiber method analysis indicate that the value of "wu" differs from the constant value assumed by Hillerborg. Furthermore, the value of "wu" for specimens with higher reinforcing ratio tends to decrease as D decreases, while those with lower reinforcing ratio tends to have approximately constant value.

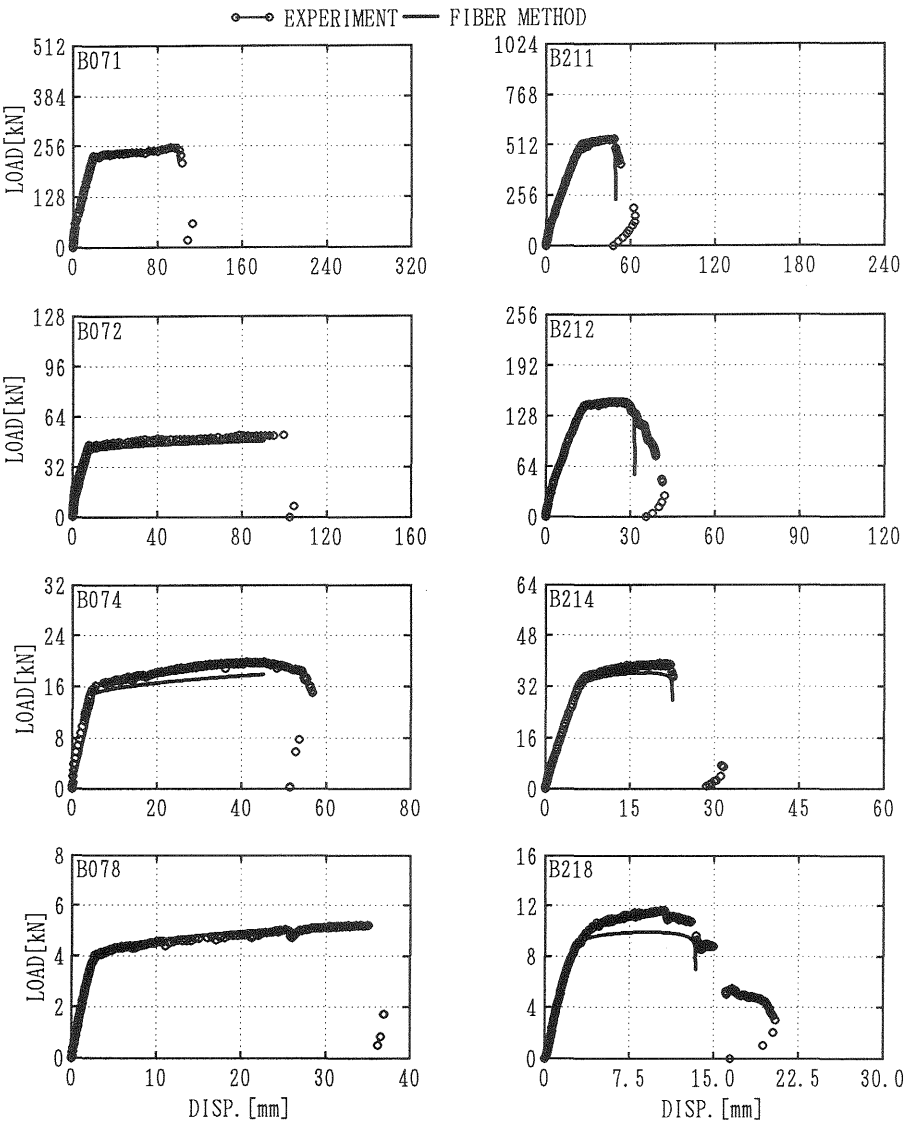

Fig.11 Comparison between experimental and analytical load-displacement curves

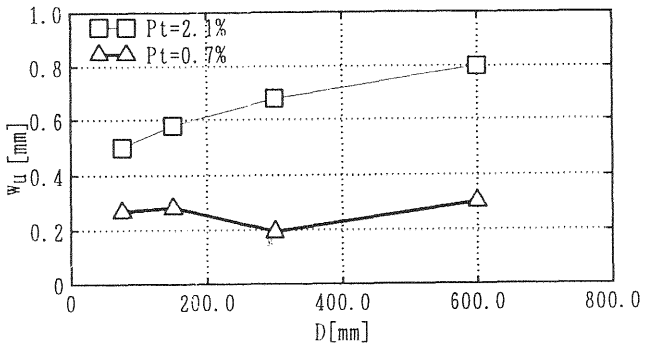

Fig.12 Relationship between best fit value of "Wu" and beam depth

5 Conclusions

Based on the analytical and test results, the following can be said:

1. Comparisons of the stress-strain curves obtained by the fiber method analysis indicate that RC beam specimens with high reinforcing ratio have more pronounced influence of size on strength, while specimens with low reinforcing ratio have more pronounced influence of size on deformability.
2. Based on the results of the four-point loading test on RC beams, it was verified that the size of the specimen has an effect on strength and deformability.
3. There is a very good agreement between the test results and the analytical results. Furthermore, the size effect on the behavior of RC beam can be clarified by adopting Hillerborg's assumption.

References

Hillerborg, A. (1988) Rotational capacity of reinforced concrete beams, **Nordic Concrete Research,** 7, 121-134

Hillerborg, A. (1989) Size dependency of the stress-strain curve in compression, in **Analysis of Concrete Structure by Fracture Mechanics** (eds L. Elfgen and S. P. Shah), ABISKO, 171-178